Biosynthesis of ternary $CuO/Co_3O_4/NiO$ nanocomposite using *jasminum mesyni* for photocatalytic and antibacterial activity

M. Zeb [a], Z. Ul Abdin [a], K. Akhter [a], Z. Anjum [b], A. Altaf [a], M. Hafeez [a,c,*]
[a] *Department of Chemistry, University of Azad Jammu & Kashmir, Muzaffarabad Pakistan*
[b] *Department of Biotechnology, University of Azad Jammu & Kashmir, Muzaffarabad, 13100, Pakistan*
[b] *Livestock & Dairy Development Department, Government of AJK, Muzaffarabad, 13100*
[c] *Faculty of Health and Life Sciences INTI International University, Persiaran Perdana BBN, Putra Nilai 71800 Nilai, Negeri Sembilan, Malaysia*

In this work, $CuO/Co_3O_4/NiO$ (CCN) NC was synthesized using an aqueous extract of *Jasminum mesyni* (*J. mesyni*) leaves which functioned as both a reducing and a capping agent. The synthesized CCN NC was characterized by various spectroscopic techniques. CCN NC demonstrated exceptional photocatalytic activity under sunlight irradiation by degrading 50 ppm aqueous methylene blue (m. blue) within 25 minutes. The kinetic studies revealed the first-order model, with a rate constant of 0.10893 min^{-1}. The bactericidal activity of CCN NC was verified against three gram-positive and three gram-negative bacteria. This study highlights the potential of CCN NC for biomedical and wastewater treatment.

(Received March 7, 2025; Accepted July 3, 2025)

Keywords: $CuO/Co_3O_4/NiO$ NC, Ternary nanocomposite, Green synthesis, Antibacterial activity, Photocatalytic activity

1. Introduction

Nanotechnology is the term used to describe the use of science to control matter at the molecular level [1]. The field of materials science and engineering is currently exploring new fundamental and applied frontiers due to the significant growth of nanotechnology. Some of these frontiers are bionanotechnology [2], nanobiotechnology [3], quantum dots [4], applied microbiology, and surface-enhanced Raman scattering [5]. Technological developments related to the setup of nanoscale structures into previously determined superstructures guarantee that nanotechnology will be indispensable in multiple key technologies. Nanotechnology is gaining significance in areas such as optics, mechanics, biomedical sciences, electronics, chemical industry, space industries, energy science, drug-gene delivery, optoelectronic devices [6,7], catalysis [8,9], nonlinear optical devices [10, 11], and photoelectrochemical applications [12, 13].

Transition metal oxide nanoparticles are being thoroughly investigated for multiple applications [14, 15, 16, 17, 18]. To improve the efficiency of these nanoparticles, researchers have modified these transition metal oxides by mixing them with other different kinds of nanoparticles. Increased surface area, surface activities, porosity, and conductivity are the distinctive characteristics that have been engendered through this modification of transition metal oxide-based nanoparticles. Furthermore, it has caused a shift in electron-hole recombination [17, 19, 20, 21, 22]. Researchers have synthesized binary, ternary, and quaternary metallic oxides-based NCs for different uses including photocatalytic and antibacterial applications. For instance, a group of researchers reported the fabrication of quaternary zinc-lead-cadmium-copper oxide NC [23]. A study reported an iron-copper oxide nanocomposite (Fe_2O_3/Cu_2O) which depicted the high stability of light-driven disintegration of the Janus green and Rhodamine-B dyes and exhibited the

* Corresponding author: muhammadhafeezchemist@gmail.com
https://doi.org/10.15251/DJNB.2025.203.707

inhibitory effect against different pathogens [24]. Another study reported the synthesis of ternary metal oxide nanomaterial NiO/Cu/CoO NC for use as an electrode [25]. One study reported the fabrication of ternary ZnO/CdO/CeO_2 heterostructure via wet chemical methods for environmental applications [26]. Similarly, Ternary Cu_2O/ZnO/Ag_3PO_4 NC was also fabricated for photocatalytic applications [27]. The literature survey shows that transition metal oxides such as CuO, NiO, and Co_3O_4 have been widely studied for different applications, whereas the comprehensive investigation of their ternary nanocomposite for both antibacterial and photocatalytic studies has not been reported yet. The current study, therefore, aims to bridge this research gap by synthesizing a CCN NC for antibacterial and photocatalytic applications.

Industrial pollutants have potentially hazardous impacts on the natural environment since they are either directly or indirectly dumped into water bodies. Untreated potentially hazardous dyes, which are released into the water from the printing, textile, and cosmetics industries lead to the contamination of the environment and cause water quality issues. These dyes have complex structures, stability, and photosensitivity. They are extremely hazardous and can cause tumors and mutagenic effects in organisms. Therefore, to create a sustainable aquatic environment, the removal of these organic pollutants from wastewater has been of paramount importance in recent years [23]. To meet this challenge, the United Nations has stressed the need for suitable water management under Sustainable Development Goal (SDG) 6, which advocates for employment of clean water technologies and pollution reduction. Nanotechnology-based methodologies offer a promising solution for this challenge by enhancing both pollutant degradation and microbial control in wastewater treatment [28]. If a single material can be used for both dye degradation and bacterial remediation, the benefits will become mutually exclusive because wastewater contains bacterial contamination along with dye pollution [23].

In this research paper, we have reported CCN NC, fabricated by the green process using an aqueous extract of *J. mesyni* leaves. This approach enhances biocompatibility, antibacterial efficiency, and wastewater treatment potential while minimizing environmental hazards and aligning with sustainable development goals. CCN NC was synthesized for the first time using *J. mesyni* leaf extract. *J. mesnyi* leaves have been selected for this research work based on their rich phytochemical profile, which includes phenols, flavonoids, and coumarins [29]. As shown by a study, the leaves have the potential to be used as an antibacterial agent [29]. The dual functionality of *J. mesyni* leaves —serving both as capping/reducing agents and as bioactive antibacterial agents—enhances the biomedical potential of the synthesized nanocomposites while supporting a sustainable, eco-friendly synthesis approach. The phase structure, purity, morphological visualization, and other spectroscopic characteristics of fabricated ternary CCN NC were studied employing X-ray diffraction (XRD), Scanning electron microscopy (SEM), Energy dispersive X-ray (EDX), Fourier-transform infrared (FTIR) spectroscopy, and Ultraviolet-visible (UV-Vis) spectroscopy. Moreover, to investigate the photocatalytic activity, the fabricated ternary nano-catalyst CCN NC was employed to degrade the organic m. blue dye. This photocatalytic test indicated that the synthesized *J. mesyni* mediated ternary CCN NC possesses a great potential to disintegrate the m. blue. The ternary CCN NC nanostructure was also verified for its bactericidal potential. The findings of the bactericidal experiment exhibited that the synthesized CCN NC can inhibit both gram-positive, and gram-negative pathogenic bacterial strains.

2. Experimental section

2.1. Preparation of leaf extract of *J. mesyni*

For extract preparation, *J. mesyni* plant leaves were collected from Muzaffarabad city, AJ&K. These leaves were rinsed thoroughly with tap water first and then with distilled water. Subsequently, drying and chopping of these leaves was carried out. 30 g of the leaves were heated (80 °C) with 500 mL distilled water for 6 hrs. During heating, continuous stirring was also applied. The light green color leaves extract obtained was filtered and then stored for synthesizing ternary CCN nano particles [30].

2.2. Synthesis of ternary CCN NC

The co-precipitation technique was utilized to fabricate the ternary CCN NC. A 50 mL aqueous solution of $Ni(NO_3)_2.6H_2O$ (0.01M), a 50 mL aqueous solution of $Cu(NO_3)_2.3H_2O$ (0.01 M), and a 50 mL aqueous solution of $Co(NO_3)_2.6H_2O$ (0.01M) were used for this synthesis. These three aqueous salt solutions were taken in a flask and 60 mL of *J. mesyni* leaf extract was added to them. The mixture of these salts solution and *J. mesyni* extract was heated (80 °C) and stirred till the appearance of precipitates which indicated the synthesis of nano-product. The CCN NC precipitates were separated, washed multiple times with distilled water, and dried in an oven at 100 °C. This dried product was crushed down into fine powder which was then calcined at 500 °C for 1.5 hours. The calcined ternary CCN NC was stored for spectroscopic characterization, antibacterial studies, and photocatalytic activity.

2.3. Characterization of CCN NC

The properties of novel ternary CCN NC were examined using different techniques such as: EDX, XRD, SEM, UV-Vis spectroscopy, and FTIR. A Shimadzu 1700 UV spectrophotometer was used to capture the UV-Vis spectrum of ternary CCN NC. To figure out the involvement of functional groups in synthesis, the FTIR spectrum in the wavelength range of 4,000-400 cm^{-1} was obtained employing the Shimadzu FTIR-8400S. The Bruker D2 Phaser served to conduct a phase study and verify the crystallinity of CCN NC. The sample was subjected to both quantitative and qualitative analysis using EDX analysis. To get morphological images of the fabricated CCN NC, SEM analysis was additionally carried out. The FEI NOVA nano SEM-450 instrument was used to capture the SEM micrograph and EDX spectrum.

2.4. Procedure of photocatalytic activity

The nanocatalyst CCN, synthesized via biological method using *J. mesyni* plant extract, was tested for its photocatalytic activity. The photocatalytic testing was conducted to degrade the organic m. blue dye. For this purpose, 30 mg of the prepared CCN NC and 50 ml of aqueous solution 50 ppm (m. blue) were taken and covered completely to carry out a dark reaction for 20 min. Subsequently, the experimental setup was moved outside in the sunlight and the cover of the reaction mixture was removed. 4 mL of the reaction mixture was drawn out at intervals of 5 min. This drawn-out mixture was evaluated by a double-beam spectrophotometer (Shimadzu 1700 UV spectrophotometer). After each time interval of 5 min, the absorbance maxima obtained was noted. The percentage degradation (% D) of the reaction was evaluated using the below formula:

$$\% D = \frac{Co - Ce}{Co} * 100 \quad (1)$$

In equation (1), C_o and C_e represent the initial concentration, and equilibrium concentration, respectively.

2.5. The procedure of antibacterial activity

CCN NC fabricated by using leaf extract of J. mesyni was substantiated for its bactericidal potential by Agar well diffusion method against both gram-positive *(S. aureus, B. subtilis,* and *S. pyogenes)* and gram-negative (*E. coli, P. mirabillis,* and *P. aurgi*nosa*)* bacterial strains. For studying the effect of ternary CCN NC concentration on antibacterial activity, four different concentrations (N1=0.2, N2=0.4, N3=0.6, and N4=0.8 mg/mL) were tested. Each concentration of CCN NC was verified three times and then the average of these three values of zone of inhibition was used for different calculations.

To carry out the antibacterial test of fabricated ternary CCN NC, nutrient broth media and Muller Hinton agar for growing culture of bacteria were utilized. A full strained loop was introduced into the nutritional broth (25 mL) for microbes transfer. These microbes were agitated at 37 °C. The culture was, subsequently, mixed with the freshly synthesized agar medium and shifted into disinfected Petri dishes which were then kept in a laminar flow for 20 min at room temperature. After solidification, 5 mm wells were set in all plates using a germ-free micropipette

tip. The agar plugs were removed with the help of sterile needles to form a well. These plates were kept in an incubator for a day and the inhibition zones appeared which were measured in mm using a scale.

2.6. Statistical analysis

Using SPSS software, a statistical analysis was conducted on the antibacterial measurements of the fabricated ternary CCN utilizing *J. mesyni* leaf extract. A 95 % Confidence Interval (CI) was established for the mean antibacterial measurements of the CCN NC against both positive and negative bacterial strains. The IC50 values were also determined for each selected pathogenic bacterial strain.

3. Results and discussion

3.1. UV-visible spectroscopy

This investigation of the fabricated ternary CCN NC showed the sensitivity of the nano-product in the UV-Vis range. The obtained absorption spectrum of synthesized CCN NC is depicted in Figure 1. Figure 1 shows the multiple bands for the synthesized CCN NC. The presence of these bands ratifies the presence of more than one metal oxide in the nano product.

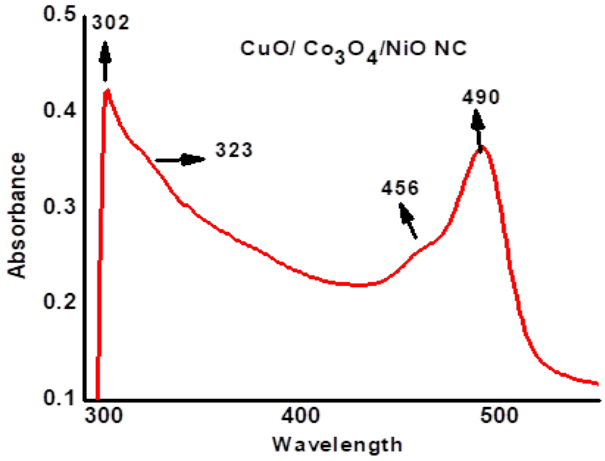

Fig. 1. UV-Vis Spectrum of ternary CCN NC.

This UV-Vis data was used for the band gap calculations also. The graph displaying the band gap of the fabricated CCN NC is presented in Figure 2. The band gap calculations were carried out using the Tauc method [31]. In this method, fitting a straight line (Tauc line), to the linear region or the steep of the optical spectrum, is done in such a way that it intersects the photon energy (hv) axis and yields the optical gap energy. The band gap energy of 2.25 eV for CCN NC indicates that the NC can absorb visible light, leading to the generation of electron-hole pair. These charge carriers can then participate in photocatalytic reactions, aiding the degradation of m. blue.

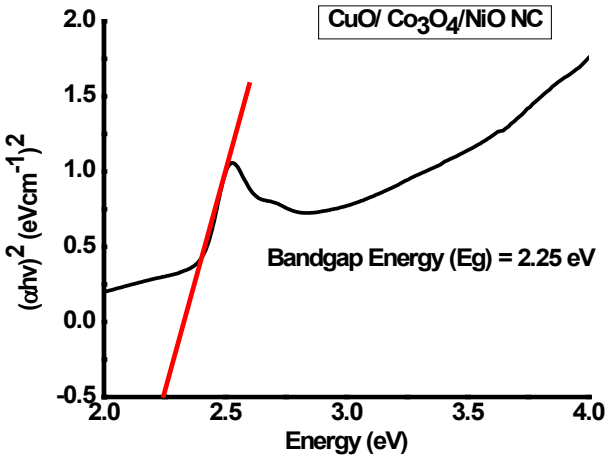

Fig. 2. The graph used for calculating bandgap using Tauc method.

3.2. Fourier transform infrared analysis

This analysis depicted the biomolecules of *J. mesyni* involved in the synthesis of the ternary CCN NC. The FTIR spectrum of the ternary CCN NC is portrayed in Figure 3. The two peaks in the obtained spectrum at 3472 cm^{-1} and 1710 cm^{-1} can be accredited to the stretching vibrations of the hydroxyl group [32] and carbonyl group, respectively. The peak at 1229 cm^{-1} can be attributed to the vibrations of -OH deformation. The peak at 1092 cm^{-1} can be assigned to the C-O group presence. The peaks for the metal-oxygen bond appear from 1000 cm^{-1} to 400 cm^{-1}. The IR spectrum of CCN NC displayed the characteristics peaks due to Co (II)-O as well as Co (III)-O at 335 and 901 cm^{-1}, respectively [33] whereas, the CuO peak is observed at 500 cm^{-1}. The existence of nickel oxide in the ternary nano-product CCN is validated by a peak around 400 cm^{-1} [34].

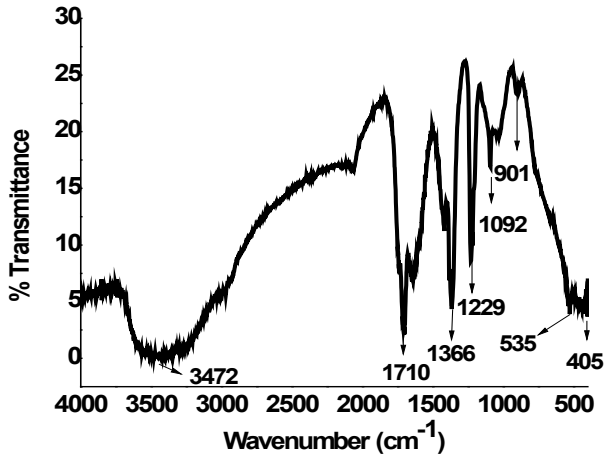

Fig. 3. IR spectrum of synthesized CCN NC.

3.3. X-ray diffraction analysis

As exhibited in the XRD pattern in Figure 4, the diffraction peaks of CuO in the fabricated ternary nanostructure were in good match with JCPDS card No. 48-1548. These peaks are present at 35°, 38°, 46°, 51.0°, 53.3°, 61°, 66°, 71°, and 73° corresponding to the (111), (111), (202), (112), (020), (113), (311), (312), and (311) matched with the CuO phase [35]. The XRD pattern represented the peaks of NiO and Co_3O_4 as well. The diffraction peaks for NiO at 43.1°, 62.6°, and 79.6° are related to the crystal planes (200), (220), and (222), respectively (JCPDS card No. 04-

835). The diffraction peaks for cobalt oxide (Co_3O_4) were also detected at 31.0°, 44.1°, 56.6°, 64.7°, 68.0°, and 77.0° which are related to planes (220), (400), (550), (422), (531), and (533) (JCPDS card No. 073–1701). From the XRD diffractogram, it is clear that the fabricated nanostructure consists of three different metallic oxides such as copper oxide, nickel oxide, and cobalt oxide as its constituents. The average crystallite size (D) of the ternary CCN NC was also calculated using the Scherrer equation, which is as follows:

$$D = (k \lambda)/\beta\cos\theta \quad (2)$$

In equation (2), λ symbolizes the X-ray wavelength and β denotes the corrected full width at half maximum of the diffraction [36, 37]. The average crystallite size of ternary CCN NC was determined to be 35.65 nm which indicates that the synthesized CCN has a high surface-to-volume ratio which can aid in its antibacterial activity.

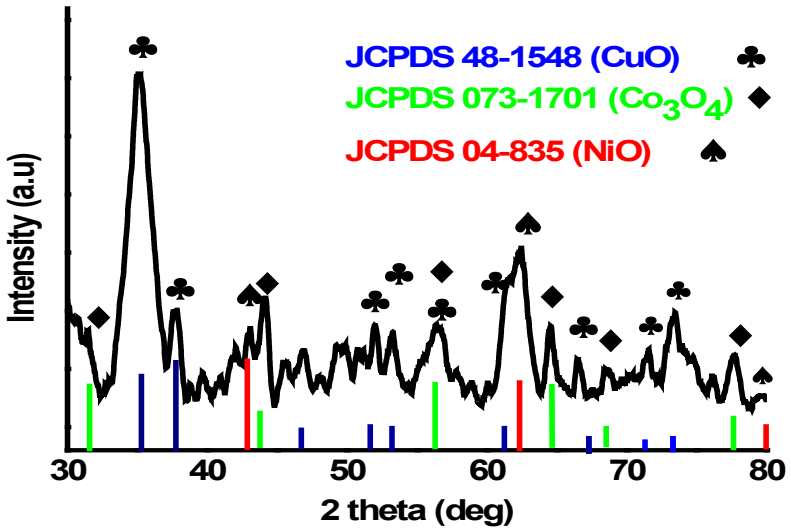

Fig. 4. XRD spectrum of CCN NC.

3.4. Energy dispersive X-ray analysis

EDX studies were also employed to reveal the profile of elements present in the fabricated CCN. Figure 5(a) depicts the EDX spectrum of the fabricated CCN NC which confirms the formation of CCN. Peaks for all four elements of the product (O, Cu, Co, and Ni) can be seen in the EDX spectrum. The composition of nickel, cobalt, copper, and oxygen in synthesized CCN NC was found to be 14.25 %, 13.01 %, 34.95 %, and 19.23 %, respectively. Small peaks for some impurities such as carbon, sulfur, phosphorous, and calcium are also visible in the spectrum of the fabricated CCN NC. These impurities are from the *J. mesyni* plant extract which is used in the synthesis of the CCN NC. The gold signal spotted in the obtained EDX spectrum is from the sample coating.

3.5. Scanning electron microscopy

The surface morphology of CCN NC fabricated using *J. mesyni* was explored via SEM analysis. The SEM image of the synthesized ternary CCN NC is depicted in Figure 5 (b). The micrograph shows elongated nanoparticles in the synthesized product. Along with this, a few spherical nanoparticles can also be seen in the micrograph. The micrograph shows that the particles of the synthesized CCN NC are packed closely to each other. Some vacant spaces are also visible in this micrograph. Overall, the particles of the ternary CCN NC are of small size and well dispersed.

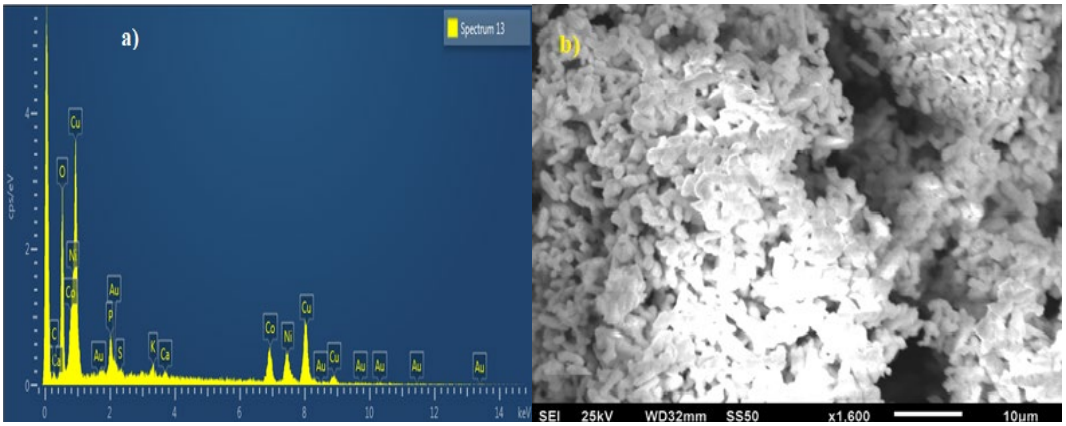

Fig. 5. (a) EDX Spectrum of synthesized CCN NC (b) SEM micrograph of synthesized CCN NC.

4. Applications of CCN NC

4.1. Photocatalytic experiment

The as-synthesized ternary CCN NC was tested for its photocatalytic potential against m. blue dye. Figure 6 exhibits the results related to this activity. In the presence of the prepared ternary CCN NC, irradiating 50 ppm aqueous solution of m. blue resulted in a lowering of absorbance with time which indicated the photodegradation of the m. blue. M. blue was found to be degraded in 25 min. Figure 6 (b) depicts the graph of the percentage degradation of m. blue dye using ternary CCN NC. The time and ln log C/C_0 plot establishes the linear relationship that shows the first-order reaction with a rate constant of 0.10893 min^{-1} Figure 6 (d).

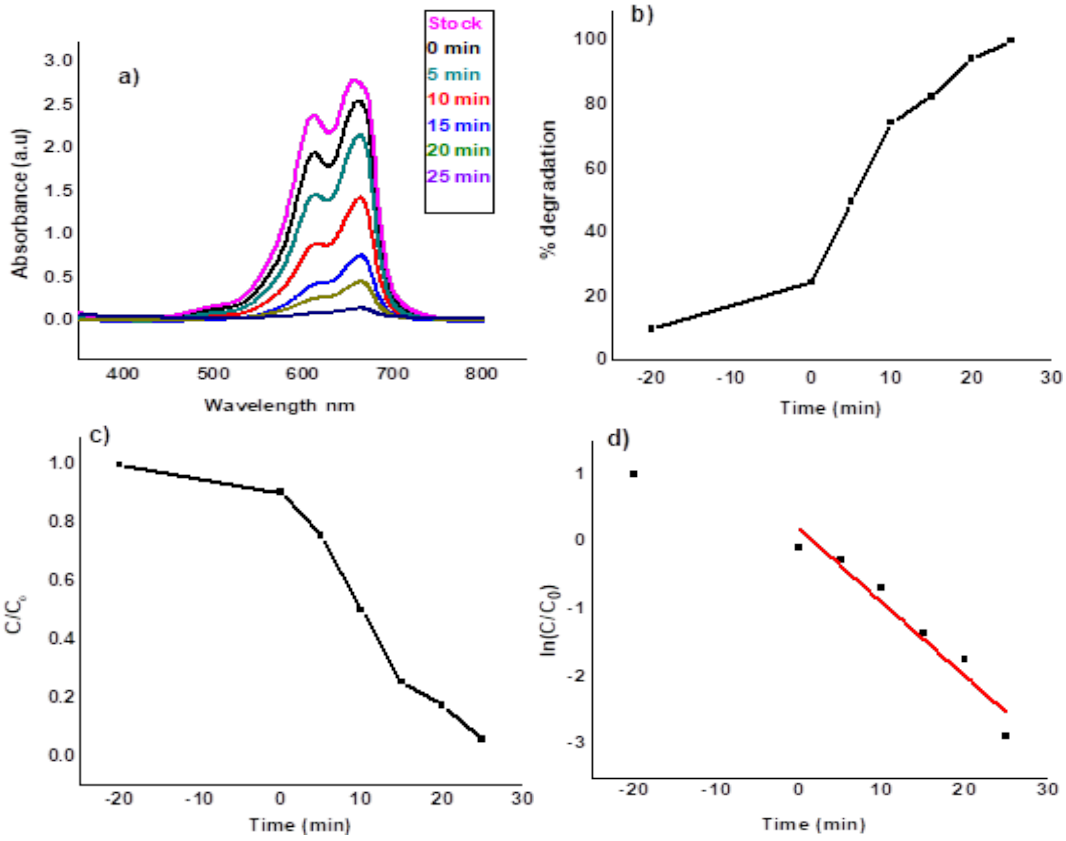

Fig. 6. Degradation profile (a) absorbance spectrum of m. blue (b) Percentage degradation with time (c) Change in absorbance maxima with time of light exposure d) Linear fitting of the absorbance spectra.

A study reported Co_3O_4 NPs synthesis using Euphorbia heterophylla which showed about 63.105 % photocatalytic degradation of m. blue in 3 hours [38]. In our recent research study, the photocatalytic activity of binary *J. mesyni* mediated Co_3O_4/NiO NC was also explored [30]. A comparison of ternary CCN NC with its binary counterpart Co_3O_4/NiO shows that CCN NC is more efficient than its binary counterpart in terms of photocatalytic activity. Binary Co_3O_4/NiO degraded 92.8 % of aqueous m. blue in 80 min as compared to the CCN NC which degraded the same dye completely within 25 min. Another study reported the synthesis of binary Co_3O_4/NiO for photocatalytic testing which showed 89.88 % degradation of aqueous m. blue in 360 min [39]. Another study reported a 93 % degradation of m. blue using Mesoporous spongy Ni-Co-oxides@wheat straw-derived SiO_2 [40]. This comparison of the photocatalytic potential of fabricated ternary CCN NC with that reported earlier shows that the *J. mesyni* mediated CCN NC is a better candidate for photocatalytic degradation of m. blue dye. This increased efficiency of the CCN NC can be attributed to the synergistic effect of leaf extract of *J. mesyni,* copper oxide, nickel oxide, and cobalt oxide.

Contact of ternary CCN NC to the sunlight triggered the stimulation of effective oxidizing agents produced on the surface of CCN which resulted in the 100 % disintegration of organic m. blue dye in 25 min. This extraordinary photocatalytic performance of ternary CCN NC can be attributed to the unique combination of three different metal oxides and *J. mesyni* leaf extract which was used in the synthesis process. The proposed mechanism of photocatalytic degradation of m. blue dye in the presence of fabricated ternary CCN NC is represented in Figure 7, which shows electronic excitation and the resultant hole (h^+) generation. The calculated band energy of 2.5 eV for CCN NC indicates that it has adequate energy to aid the formation of reactive oxygen species (ROS). This energy is comparable to that required for the generation of hydroxyl and superoxide radicals, which are key ROS species involved in photocatalytic degradation.

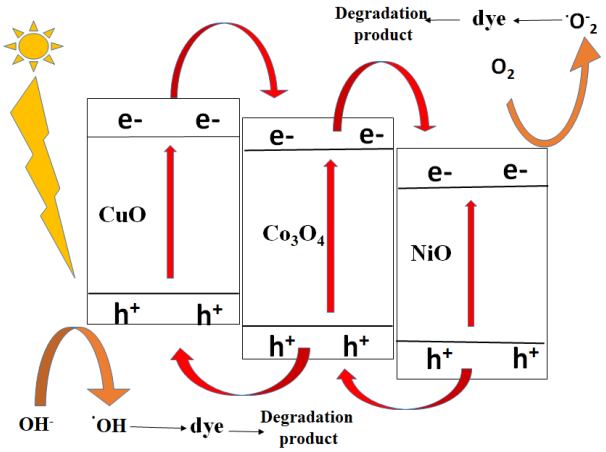

Fig. 7. Mechanism of photocatalytic activity of ternary CCN NC synthesized using J. mesyni leaf extract.

4.2. Antibacterial activity

Ternary CCN NC, fabricated by employing leaf extract of *J. mesyni* leaves, was utilized to test its antibacterial potential against the selected pathogenic bacterial strains. The values of bactericidal measurements of fabricated ternary NC are enlisted in Table 1. The results validated that the ternary CCN NC has great potential as an inhibitory agent against different pathogens. It was observed that the inhibitory action increased as the concentration of the nanomaterial was increased.

For P. aurginosa and P. mirabillis, the CCN NC showed a maximal inhibitory efficacy (33 mm) whereas for *P. aurgi*nosa, the ternary NC showed the minimum inhibitory efficacy (2 mm) at 0.2 mg against *P. aurgi*nosa. Furthermore, a 95 % CI for the mean antibacterial activity was also

computed. The IC50 values were also calculated for the bactericidal measurements of ternary NC against each selected pathogenic bacterial strain. The range of IC50 values of CCN NC is between 8.0 and 33.0 mg/mL. Figure 6 shows the images of the antibacterial measurements of fabricated ternary CCN NC.

A comparison of the antibacterial activities of fabricated CCN NC with previously synthesized ternary, binary, and single nanomaterials shows that CCN NC is a superior antibacterial agent. For instance, a group of researchers synthesized a ternary Cu−Ni−Zn oxide NC using a green method and tested this NC against two pathogens such as *S. aureus* and *E. coli.* They observed a maximum ZOI of 25 mm against *S. aureaus* [41], whereas the synthesized CCN NC showed a zone of inhibition of 33 mm. In another study, 20 % nickel-doped cobalt oxide nanoparticles showed a ZOI of 20 mm against *E. coli,* 18 mm against *B. subtilis*, 14 mm against *P. aeruginosa*, and 13 mm against *S. aureaus* [42].

The average crystallite size of ternary CCN NC was determined to be 35.65 nm which indicates that the synthesized CCN has a high surface-to-volume ratio, which enables it to penetrate and cause damage to the cell membrane. Furthermore, this high surface area can also lead to an increased reactivity and interaction with bacterial cell, potentially increasing the inhibitory effect of the synthesized CCN NC. Another factor contributing to the superior antibacterial activity of the CCN NC can be the synergistic effect of the *J. mesyni* leaf extract and the oxides of Cu, Co, and Ni.

Table 1. Antimicrobial activity of CCN NC against the selected pathogenic bacteria.

Bacteria	ZOI (mm)				Standard Deviation	Mean activity (95% CI)	IC50 values (mg/mL)
	N1	N2	N3	N4			
S. aureus	17.3	22.3	33.0	33.0	7.8	26.4±7.7	16.5
S. pyogenes	15.3	26.0	30.6	32.0	7.5	25.9±7.4	24.6
B. subtilis	17.0	20.3	22.3	24.6	3.2	21.0 ±3.1	19.0
E. coli	9.0	15.3	19.0	19.3	4.7	15.6±4.7	16.2
P. mirabillis	31.6	33.0	33.0	33.0	16.1	24.4±15.8	8.0
*P. aurg*inosa	2.00	18.00	33.00	33.00	14.7	21.5±14.50	33.3

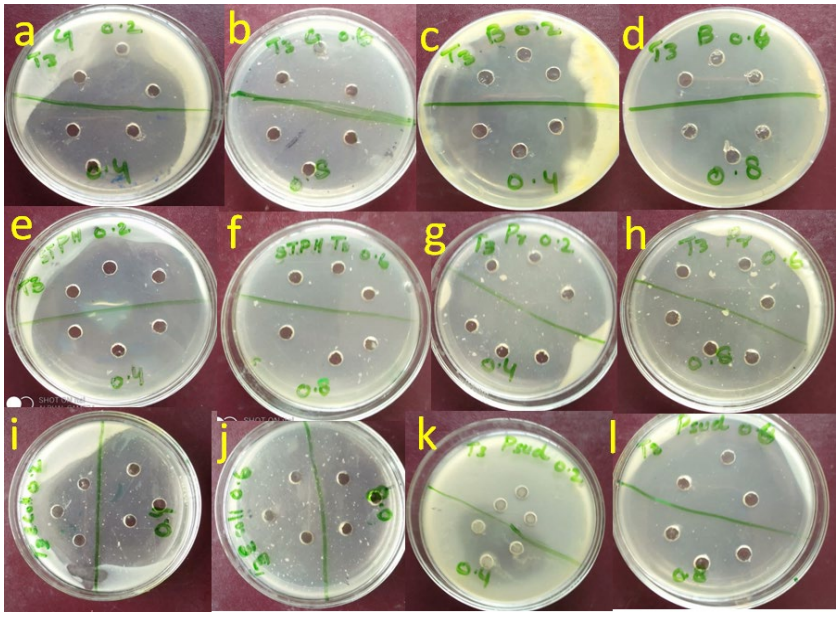

Fig. 8. Antibacterial measurements of CCN NC.

5. Conclusion

In summary, ternary CCN NC was successfully synthesized by a green method using *J. mesyni* leaf extract. The optical properties, morphological characteristics, phase constitution, and elemental composition of fabricated CCN NC were studied using various characterization techniques. The synthesized CCN NC was tested for its antibacterial as well as photocatalytic activities. The result of photocatalytic activity of CCN NC against m. blue showed that it is an efficient nano-catalyst and is far better than its binary counterpart synthesized under similar conditions. It degraded the 50 ppm of m. blue within 25 minutes. The result of antibacterial activity showed that the synthesized CCN NC depicted an excellent inhibitory effect against gram-positive as well as gram-negative pathogenic bacteria.

References

[1] S. Senapati, Biosynthesis and immobilization of nanoparticles and their applications. (2005)

[2] D. S. Goodsell, Bionanotechnology: lessons from nature. John Wiley & Sons. (2004); https://doi.org/10.1002/0471469572

[3] H. Klefenz, Engineering in life sciences 4(3), 211-218 (2004); https://doi.org/10.1002/elsc.200402090

[4] W. C. Chan, S. Nie, Science 281(5385), 2016-2018 (1998); https://doi.org/10.1126/science.281.5385.2016

[5] Z. Q. Tian, B. Ren, Annual Review of Physical Chemistry 55(1), 197-229 (2004); https://doi.org/10.1146/annurev.physchem.54.011002.103833

[6] V. L. Colvin, M.C. Schlamp, A. P. Alivisatos, Nature 370(6488), 354-357 (1994); https://doi.org/10.1038/370354a0

[7] Y. Wang, N. Herron, The Journal of Physical Chemistry, 95(2), 525-532 (1991); https://doi.org/10.1021/j100155a009

[8] G. Schmid, Chemical reviews 92(8), 1709-1727 (1992); https://doi.org/10.1021/cr00016a002

[9] A. J. Hoffman, G. Mills, H. Yee, M. R. Hoffmann, The Journal of Physical Chemistry 96(13), 5546-5552 (1992); https://doi.org/10.1021/j100192a067

[10] A. D. Yoffe, Adv. Advances in Physics 42(2), 173-262 (1993); https://doi.org/10.1080/00018739300101484

[11] Y. Wang, Accounts of Chemical Research 24(5), 133-139 (1991); https://doi.org/10.1021/ar00005a002

[12] H. S. Mansur, F. Grieser, M. S. Marychurch, S. Biggs, R. S. Urquhart, D. N. Furlong, Journal of the Chemical Society, Faraday Transactions 91(4), 665-672 (1995); https://doi.org/10.1039/FT9959100665

[13] S. Iravani, Green chemistry 13(10), 2638-2650 (2011); https://doi.org/10.1039/c1gc15386b

[14] N. Rani, M. Saini, S. Yadav, K. Gupta, K. Saini, M. Khanuja, AIP Conference Proceedings 2276(1) (2020). AIP Publishing.

[15] F. Pino, C. C. Mayorga-Martinez, A. Merkoçi, Electrochemistry Communications, 71, 33-37 (2016); https://doi.org/10.1016/j.elecom.2016.08.001

[16] A. Aboulouard, B. Gultekin, M. Can, M. Erol, A. Jouaiti, B. Elhadadi, S. Demic, Journal of Materials Research and Technology 9(2), 1569-1577 (2020); https://doi.org/10.1016/j.jmrt.2019.11.083

[17] S. Bhatia, N. Verma, Mater Materials Research Bulletin 95, 468-476 (2017); https://doi.org/10.1016/j.materresbull.2017.08.019

[18] M. S. S. Danish, L.L. Estrella, I. M. A. Alemaida, A. Lisin, N. Moiseev, M. Ahmadi, T. Senjyu, Metals 11(1), 80 (2021); https://doi.org/10.3390/met11010080

[19] S. Thambidurai, P. Gowthaman, M. Venkatachalam, S. Suresh, Journal of Alloys and Compounds 830, 154642 (2020); https://doi.org/10.1016/j.jallcom.2020.154642

[20] T. Jan, S. Azmat, Q. Mansoor, H. M. Waqas, M. Adil, S. Z. Ilyas, M. Ismail, Microbial pathogenesis 134, 103579 (2019); https://doi.org/10.1016/j.micpath.2019.103579

[21] M. Dutt, A. Ratan, M. Tomar, V. Gupta, V. Singh, Journal of Physics and Chemistry of Solids 145, 109536 (2020); https://doi.org/10.1016/j.jpcs.2020.109536

[22] S. Yadav, N. Rani, K. Saini, Materials Science and Engineering 1225(1), 012004 (2022); https://doi.org/10.1088/1757-899X/1225/1/012004

[23] G. Murugadoss, K. Thiruppathi, N. Venkatesh, S. Hazra, A. Mohankumar, G. Thiruppathi, P. Sakthivel, Journal of Environmental Chemical Engineering 10(1), 106961 (2022); https://doi.org/10.1016/j.jece.2021.106961

[24] M. R. Abhilash, G. Akshatha, S. Srikantaswamy, RSC advances, 9(15), 8557-8568 (2019); https://doi.org/10.1039/C8RA09929D

[25] M. Manikandan, E. Manikandan, V. Swetha, S. Kurpaa, S. Vijay, V. Kiruthika, Scientific Reports, 14(1), 10821(2024); https://doi.org/10.1038/s41598-024-61625-y

[26] M. Ishfaq, W. Hassan, M. Sabir, H. Somaily, S. K. Hachim, Z. J. Kadhim, M. Aadil, Ceramics International, 48(23), 34590-34601 (2022); https://doi.org/10.1016/j.ceramint.2022.08.046

[27] A. M. Taddesse, M. Alemu, T. Kebede, Journal of Environmental Chemical Engineering 8(5), 104356 (2020); https://doi.org/10.1016/j.jece.2020.104356

[28] B. Elzein, Heliyon 10(10), (2024); https://doi.org/10.1016/j.heliyon.2024.e31393

[29] R. Verma, B. S. Balaji, A. Dixit, Bioinformation 14, 430(2018); https://doi.org/10.6026/97320630014430

[30] M. Zeb, Z. Anjum, S. Mumtaz, M. Khalid, M. Hafeez, Desalination and Water Treatment, 317, 100165 (2024); https://doi.org/10.1016/j.dwt.2024.100165

[31] S. Yasmeen, F. Iqbal, T. Munawar, M. A. Nawaz, M. Asghar, A. Hussain, Ceramics International 45(14), 17859-17873 (2019); https://doi.org/10.1016/j.ceramint.2019.06.001

[32] E. A. Aboelazm, G. A. Ali, K. F. Chong, Chemistry of Advanced Materials 3(4), 67-73 (2018)

[33] M. Samer, E. M. Abdelsalam, S. Mohamed, H. Elsayed, Y. Attia, Environment, Development and Sustainability 1-18(2021)

[34] Y. Ren, L. Gao, Journal of the American Ceramic Society, 93(11), 3560-3564 (2010); https://doi.org/10.1111/j.1551-2916.2010.04090.x

[35] S. Chabri, A. Dhara, B. Show, D. Adak, A. Sinha, N. Mukherjee. Catalysis Science & Technology, 6(9), 3238-3252 (2016); https://doi.org/10.1039/C5CY01573A

[36] L. Takacs, Chemical Society Reviews, 42(18), 7649-7659 (2013); https://doi.org/10.1039/c2cs35442j

[37] Q. Zhang, Y. Xie, F. Ling, Z. Song, D. Li, Y. Lu, ... X. Zhou. Vacuum 196, 110764 (2022); https://doi.org/10.1016/j.vacuum.2021.110764

[38] N. O. M. Dewi, Y. Yulizar, D. B: Materials Science and Engineering 509(1), 012105 (2019); https://doi.org/10.1088/1757-899X/509/1/012105

[39] S. Yadav, J. Yadav, M. Kumar, K. Saini, International Journal of Hydrogen Energy 47(99), 41684-41697 (2022); https://doi.org/10.1016/j.ijhydene.2022.02.011

[40] M. A. Hussein, M. M. Motawea, M. M. Elsenety, S. M. El-Bahy, H. Gomaa, Applied Nanoscience 12(5)1519-1536 (2022); https://doi.org/10.1007/s13204-021-02318-0

[41] J. Khan, S. Bibi, I. Naseem, S. Ahmed, M. Hafeez, K. Ahmed, L. Tao, ACS omega 8(23), 21032-21041 (2023); https://doi.org/10.1021/acsomega.3c01896

[42] M. Mayakannan, S. Gopinath, S. Vetrivel, Materials Chemistry and Physics 242, 122282 (2020); https://doi.org/10.1016/j.matchemphys.2019.122282